Targeted expression of the inositol 1,4,5-triphosphate receptor (IP_3R) ligand-binding domain releases Ca^{2+} via endogenous IP_3R channels

Péter Várnai*, András Balla†, László Hunyady*, and Tamas Balla†‡

†Endocrinology and Reproduction Research Branch, National Institute of Child Health and Human Development, National Institutes of Health, Bethesda, MD 20892; and *Department of Physiology, Faculty of Medicine, Semmelweis University, 1085 Budapest, Hungary

Edited by Clara Franzini-Armstrong, University of Pennsylvania School of Medicine, Philadelphia, PA, and approved April 7, 2005 (received for review October 11, 2004)

Virtually all functions of a cell are influenced by cytoplasmic [Ca^{2+}] increases. Inositol 1,4,5-trisphosphate receptor (IP_3R) channels, located in the endoplasmic reticulum (ER), release Ca^{2+} in response to binding of the second messenger, IP_3. IP_3Rs thus are part of the information chain interpreting external signals and transforming them into cytoplasmic Ca^{2+} transients. IP_3Rs function as tetramers, each unit comprising an N-terminal ligand-binding domain (LBD) and a C-terminal channel domain linked by a long regulatory region. It is not yet understood how the binding of IP_3 to the LBD regulates the gating properties of the channel. Here, we use the expression of IP_3 binding protein domains tethered to the surface of the endoplasmic reticulum (ER) to show that the all-helical domain of the IP_3R LBD is capable of depleting the ER Ca^{2+} pools by opening the endogenous IP_3Rs, even without IP_3 binding. This effect requires the domain to be within 50 Å of the ER membrane and is impaired by the presence of the N-terminal inhibitory segment on the LBD. These findings raise the possibility that the helical domain of the LBD functions as an effector module possibly interacting with the channel domain, thereby being part of the gating mechanisms by which the IP_3-induced conformational change within the LBD regulates Ca^{2+} release.

Ca^{2+} channel | endoplasmic reticulum | red fluorescent protein

The intracellular second messenger, inositol 1,4,5-trisphosphate (IP_3) is generated upon stimulation of cell-surface receptors linked to phospholipase C (PLC) activation (1). IP_3 rapidly binds to an intracellular receptor and releases Ca^{2+} from intracellular Ca^{2+} stores; hence, both IP_3 and its receptor (IP_3R) are key components of the signal transduction mechanism that links cell-surface receptors to calcium-regulated intracellular responses (2). All three isoforms of the IP_3R (types I, II, and III) function as intracellular Ca^{2+} channels that work as homotetramers or heterotetramers (3). Each receptor subunit has a channel portion containing six transmembrane helices and a pore domain located between TM5 and TM6, close to the C terminus of the protein (4–6). The ligand-binding domain (LBD) of the receptor is located at the N terminus (7) and is separated from the channel domain by a long intervening regulatory region facing the cytoplasm (3, 7). IP_3 binding leads to rapid activation of the channel, but Ca^{2+}-induced Ca^{2+} release, similar to that characteristic of the related ryanodine receptors (RyRs), has also been recognized as an important regulatory feature of IP_3Rs (8). Because of this complex, and often subtype-specific, regulation of IP_3 channels, cells can display complex Ca^{2+} wave patterns and oscillations after agonist stimulation, the shape and frequency of which can have unique importance in the selective regulation of downstream effectors (9–11).

Despite intense studies, little is known about the manner in which the binding of IP_3 to the N-terminal LBD affects the channel gating properties of the molecule. Upon IP_3 binding, the LBD undergoes a significant conformational change as evidenced by the IP_3-induced alteration of its migration on a size-exclusion column (7) and by its suitability as a FRET-based sensor of IP_3 binding (12). As shown recently, the C-terminal channel domain, isolated from the rest of the receptor, is constitutively active, and the presence of the regulatory domain is required to maintain the suppression of channel activity (13, 14). Moreover, elegant cross-linking experiments have shown that the N-terminal domain of the receptor is in juxtaposition with the C-terminal channel domain (15). These data together raised the possibility that the proximity of the LBD to the channel domain may be an important aspect of IP_3R regulation after binding of IP_3. The present study was designed to investigate whether the LBD of the IP_3R acts as a tethered regulatory module that regulates the channel activity via IP_3-induced conformational changes. For this purpose, we used a molecular approach by which the isolated LBD of type I IP_3R or its components was tethered to the cytoplasmic surface of the endoplasmic reticulum (ER), and the effects of their expression on Ca^{2+} signaling was compared with those of the same constructs expressed in the cytoplasm. These experiments revealed that the all-helical domain of the LBD is capable of opening the IP_3R and suggest that the IP_3-induced conformational change may involve the unmasking of this domain for interaction with other portions of the molecule, possibly with the channel domain.

CELL BIOLOGY

Materials and Methods

DNA Constructs. The construction of rat p130PH and the LBD of human type 1 IP_3R (224–605) fused to the C-terminal of GFP have been described (16). The same constructs were also created fused to monomeric red fluorescent protein (mRFP) by exchanging the GFP coding sequence with that of mRFP (17). Mutant forms of the constructs (p130PH R134L and IP_3R-224–605 K508A were generated by using the QuikChange mutagenesis kit (Stratagene). For ER tethering, the C-terminal ER localization sequence (MVYIGIAIFLFVGLFMK) of the yeast UBC6 protein (X73234, residues 233–250) was fused to the C termini of the constructs through a short linker (NSRV). The long rigid helical linker built between the ER localization sequence and the LBD contained 9x(EAAAR) residues and was synthesized as double-stranded DNA with EcoRI restriction sites at both ends (Blue Heron Biotechnology, Bothell, WA). The ER lumen-targeted protein coded by the pEF/Myc/ER/GFP vector (Invitrogen) was used to visualize the ER. The design, production, and purification of recombinant proteins, as well as the IP_3 binding assays performed on them, have been described (16).

This paper was submitted directly (Track II) to the PNAS office.

Abbreviations: IP_3, inositol 1,4,5-trisphosphate; IP_3R, IP_3 receptor; LBD, ligand-binding domain; RyR, ryanodine receptor; ER, endoplasmic reticulum; mRFP, monomeric red fluorescent protein; PH, pleckstrin homology; Tg, thapsigargin; TKO triple knockout.

‡To whom correspondence should be addressed at: National Institutes of Health, Building 49, Room 6A35, 49 Convent Drive, Bethesda, MD 20892-4510. E-mail: tambal@box-t.nih.gov.

Cytoplasmic Ca^{2+} Measurements. COS-7 cells were cultured on glass coverslips (3×10^5 cells per 35-mm dish) and transfected with the various constructs (2 μg per dish) by using Lipofectamine 2000 for 24 h as described in ref. 16. For calcium measurements, cells were loaded with Fura-2/AM (2 μM, 45 min; Molecular Probes). DT40 cells [wild-type or triple knockout (TKO)] were transfected with plasmid DNA (15 μg) by using electroporation [10^7 cells per 0.5 ml of OPTI-MEM (Invitrogen) 290 V, 28 ms] with a BTX (San Diego) T 820 electroporator. One day after transfection, cells were transferred to glass coverslips precoated with Cell-Tak (Collaborative BioMedical Products, Bedford, MA) and loaded with Fura-2/AM (2 μM, 30 min). Single-cell calcium measurements were performed at room temperature in a modified Krebs–Ringer buffer containing 120 mM NaCl, 4.7 mM KCl, 1.2 mM $CaCl_2$, 0.7 mM $MgSO_4$, 10 mM glucose, and 10 mM Na-Hepes at pH 7.4. An Olympus (Melville, NY) IX70 inverted microscope equipped with a Lambda DG-4 (Sutter Instruments, Novato, CA) illuminator and an ORCA-ER (Hamamatsu, Hamamatsu City, Japan) or MicroMAX:1024BFT (Princeton Instruments, Trenton, NJ) digital camera and the appropriate filter sets were used for Ca^{2+} analysis. Data acquisition and processing were performed by using METAFLUOR software (Universal Imaging, Downington, PA). Calcium measurement in populations of DT40 cells (10^6 cells per ml) was performed in a fluorescence spectrophotometer (DeltaScan, PTI, Lawrenceville, NJ) after loading with Fura-2/AM (2 μM, 45 min). The localization of the ER-tethered constructs was determined by confocal microscopy as detailed elsewhere (16).

Mn^{2+} Quench Experiments. COS-7 cells cultured on glass coverslips were loaded with Fura-2/AM (5 μM, 120 min) at room temperature. Cells were permeabilized with 15 μg/ml digitonin for 10 min in an intracellular medium [10 mM NaCl, 120 mM KCl, 2.2 mM $MgCl_2$, 1 mM $KHPO_4$, 20 mM Hepes (pH 7.2), and Ca^{2+} depleted by Chelex 100 (Bio-Rad) treatment] supplemented with 2 mM ATP, 10 mM phosphocreatine, and 20 units/ml creatine phosphokinase. Single-cell fluorescence measurements were performed at room temperature in the above microscope system by using 360 nm as the excitation wavelength.

Results and Discussion

Cytoplasmic Expression of IP_3 Binding Domains Alters Agonist-Induced Ca^{2+} Signaling. The N-terminal IP_3 binding region (224–605) of the type I IP_3R or the pleckstrin homology (PH) domain of the phospholipase C (PLC)-like p130 protein (18) was fused to the mRFP for expression in COS-7 cells. The latter was used as a control, because it also binds IP_3, although with somewhat lower affinity, but bears no structural homology to the IP_3R LBD (16). Fusion of these domains to fluorescent proteins allowed monitoring of both the expression levels and the localization of the proteins simultaneously with cytoplasmic Ca^{2+} measurements with Fura-2. As shown in Fig. 1*A*, consistent with earlier studies (18, 19), cytoplasmic expression of either the ligand-binding segment of IP_3R (224–605) (IP_3R LBD) or p130PH caused a dose-dependent delay in the onset and the peak of the cytoplasmic Ca^{2+} increase in response to stimulation of the endogenous P_{2y} purinergic receptors by ATP. When the Ca^{2+} peak delays were plotted against the fluorescence intensities for each individual cell expressing one of the two IP_3-binding proteins, the different IP_3 affinities of the two domains were clearly reflected in their efficacies in delaying the Ca^{2+} responses (Fig. 1*B*). The delayed and less "synchronized" Ca^{2+} increases appeared as a blunted Ca^{2+} response in the averaged Ca^{2+} traces, which also show that mutant forms of either domain (R134L of p130PH or K508A of IP_3R LBD) that did not bind IP_3 had no significant effect on the Ca^{2+} responses (Fig. 1 *B* and *C*). These data were all consistent with the ability of these domains to bind IP_3 within its physiological concentration range and buffer IP_3 increases with the expected consequences on Ca^{2+} signaling.

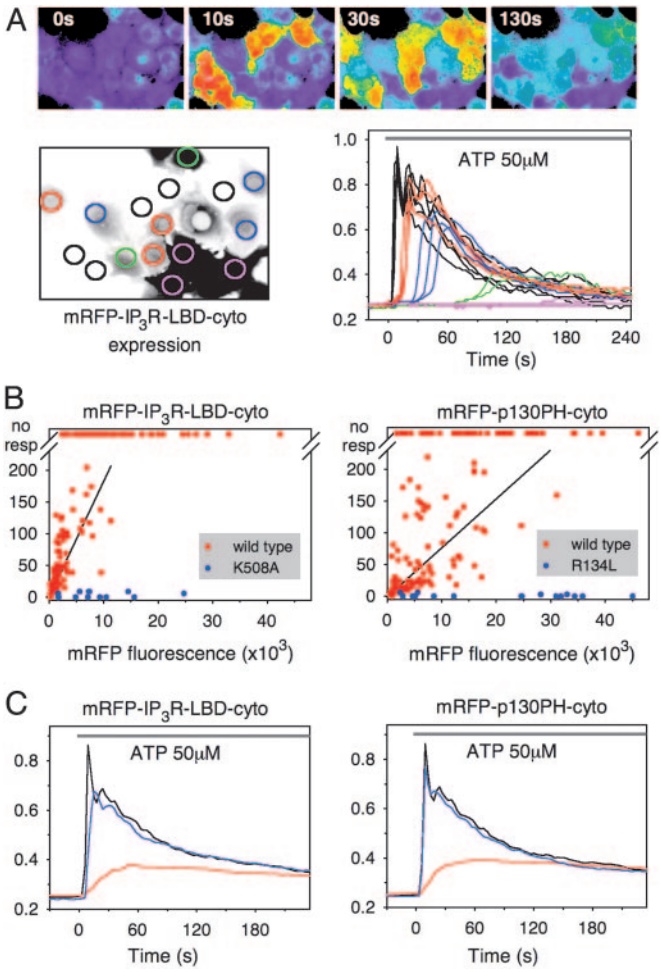

Fig. 1. Inhibition of agonist-induced Ca^{2+} signaling by overexpressed IP_3-binding domains. (*A*) COS-7 cells were transfected with IP_3R LBD (224–605) fused to the C terminus of mRFP. After 24 h, cells were loaded with Fura-2 and stimulated by 50 μM ATP at time 0. The cytoplasmic [Ca^{2+}] responses of the individual cells from a visual field containing cells expressing various levels of IP_3R LBD are shown (*Upper*) as assessed by mRFP fluorescence (shown *Lower Left*). The kinetics of the [Ca^{2+}] responses of the individual cells (color-coded red, blue, green, and pink to reflect increasing expression levels) are shown *Lower Right*. cyto, Cytoplasmic. (*B*) The peak of the cytoplasmic [Ca^{2+}] response is delayed as a function of the expression level of the indicated IP_3 binding domain. Cells without a measurable [Ca^{2+}] response within 4 min are plotted at the top (no resp). Blue dots indicate cells expressing mutant constructs incapable of IP_3 binding. Note the difference between the potencies of the IP_3R LBD and p130PH proteins (slopes of the fitted data, 18.3×10^{-3} and 7.7×10^{-3}; $r^2 = 0.467$ and $r^2 = 0.261$, respectively; $P < 0.001$ in both cases) reflecting the difference in their IP_3 affinities (16). (*C*) Summary of Ca^{2+} responses after averaging the individual responses shown in *B* and using the same color-coding. The Ca^{2+} response of untransfected cells is shown by the black traces.

ER-Tethered IP_3R LBD Impairs Ca^{2+} Signaling by Depleting the ER Ca^{2+} Stores Independent of IP_3 Binding. Next, the same domains were tethered to the outer surface of the ER by the addition of a short hydrophobic C-terminal ER-targeting sequence from the yeast UBC6 protein (20) (Fig. 2*A*). Expression of the p130PH-ER construct exerted effects on Ca^{2+} signaling that were very to similar to those of its cytosolic version and required the construct to bind IP_3 (Fig. 2*B Right*). In contrast, although the IP_3R LBD-ER construct also exerted a strong inhibition on the

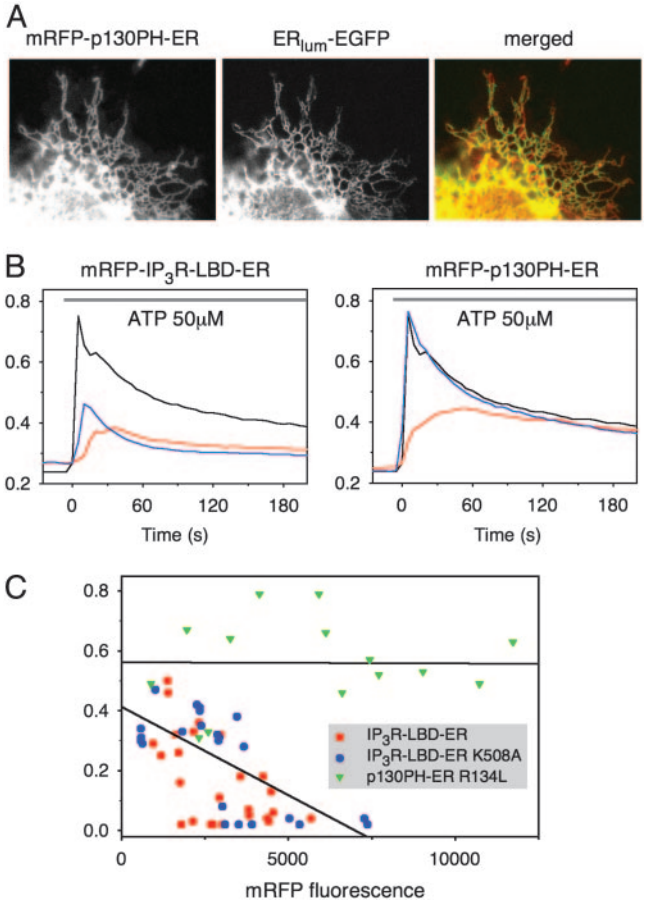

Fig. 2. Expression of ER-tethered IP_3 binding domains and their effects on Ca^{2+} signaling. (*A*) Colocalization of mRFP p130PH tethered to the surface of the ER with a luminally ER-targeted GFP. (*B*) Averaged Ca^{2+} responses of cells expressing similar levels of the ER-tethered domains (red traces) or their mutant forms (blue traces) and the untransfected cells (black traces). Note that in the case of the IP_3R LBD-ER (*Left*), the [Ca^{2+}] response is greatly affected even when the mutant form is expressed, whereas, in the case of the p130PH-ER protein (*Right*), only the wild-type with IP_3 binding exerts an effect. (*C*) Although there is no delay in the peak [Ca^{2+}] response with the mutant IP_3R LBD-ER, the amplitude of the response is reduced in the case of both the wild-type (red dots) and the mutant (blue dots) IP_3R LBD-ER protein as a function of expression level, whereas the mutant p130PH-ER (green triangles) is without effect.

ATP-induced Ca^{2+} increase, its mutant form was as effective as the wild-type to inhibit the Ca^{2+} signal, except that, in the case of the mutant, the smaller Ca^{2+} response was not associated with a delay (Fig. 2*B Left*). The amount of Ca^{2+} released by the agonist was progressively decreased by increasing the expression of either the wild-type or the K508A mutant of the IP_3R LBD ER but not of the mutant p130PH-ER construct (Fig. 2*C*) (note that the fluorescence intensity range is narrower with the ER-tethered constructs). This finding raised the possibility that the ER Ca^{2+} pools are depleted in the cells expressing these constructs. To determine the extent of store depletion, the ability of the sarco(endo)plasmic reticulum Ca^{2+} ATPase (SERCA) inhibitor thapsigargin (Tg) to empty the IP_3-sensitive Ca^{2+} stores (21) was examined. As shown in Fig. 3*A*, the cytoplasmic Ca^{2+} increase evoked by Tg was greatly diminished in cells expressing the ER-targeted IP_3R LBD. Importantly, again, the mutant form of IP_3R LBD ER, unable to bind IP_3, was as effective as the wild-type form in emptying the ER Ca^{2+} stores (Fig. 3*A Left*). Neither the wild-type nor the mutant IP_3R LBD affected the Tg-induced Ca^{2+} response when expressed in the cytosol (Fig. 3*A Center*), and the ER-targeted p130PH was also without effect (Fig. 3*A Right*). Similar results were obtained when the Ca^{2+} stores were emptied in Ca^{2+}-free medium either with the Ca^{2+} ionophore, ionomycin, or Tg (Fig. 3*B Center* and *Right*, respectively). The Ca^{2+} response to the IP_3-sensitizing agent, thimerosal, was also largely diminished by the ER-targeted IP_3R LBD (Fig. 3*B Left*).

If the Ca^{2+} stores are depleted, cells should display an increased Ca^{2+} influx due to the activation of the store-operated Ca^{2+} entry pathway (22). Therefore, the response of cells to the extracellular addition of Ca^{2+} after a short Ca^{2+}-free incubation was examined. As shown in Fig. 3*C*, cells expressing the ER-tethered IP_3R LBD construct, but not its cytosolic form or the p130PH-ER construct, showed enhanced Ca^{2+} increase after Ca^{2+} addition, consistent with the activated Ca^{2+} entry pathway secondary to depleted Ca^{2+} stores. This enhanced Ca^{2+} entry was similar to, although more transient than, that observed in normal cells after depleting the Ca^{2+} stores with Tg (Fig. 3*B Right*). The effects of an activated capacitative Ca^{2+} entry pathway were also reflected in the elevated basal Ca^{2+} levels in the cells expressing the ER-tethered IP_3R LBD in the presence of Ca^{2+} (Figs. 2*B Left* and 3*A Left*) and its decrease in the absence of external Ca^{2+} (Fig. 3*B Center* and *Right*). This Ca^{2+} elevation, however, was relatively moderate compared with that observed after an acute emptying of the Ca^{2+} stores, which probably reflects the activation of compensatory mechanism(s) to protect the cells from flooding with Ca^{2+} as has been observed when Ca^{2+} stores were emptied by the expression of leaky IP_3R channels (14).

To assess the conductivity of the IP_3R more directly, we used the Mn^{2+}-quench method in single permeabilized COS-7 cells (23). In this method the cells are loaded with Fura-2 under conditions that favor the loading of the probe into the organelles, and, after permeabilizing and washing out the cytosolic component of Fura-2, the addition of Mn^{2+} quenches the luminal fluorescence partially by entering through IP_3Rs (24). As shown in Fig. 3*D*, the addition of Mn^{2+} to permeabilized COS-7 cells caused a gradual decrease in the Fura-2 fluorescence (measured by exciting at the Ca^{2+} insensitive wavelength of 360 nm) that was similar in naive cells and in the cells expressing the p130PH-ER construct. In both cases this basal rate of quenching was rapidly increased upon addition of 3 μM IP_3 to the cells. In contrast, the rate of initial Mn^{2+} quench was significantly larger, and there was no effect of IP_3 in the cells expressing the IP_3R LBD K508A ER (or the wild-type form; data not shown). These data were also consistent with the open state of the IP_3R in the COS-7 cells expressing the ER-targeted IP_3R LBD.

ER-Tethered IP_3R LBD Depletes the ER Ca^{2+} Stores via Endogenous IP_3 Receptors. To determine further whether the tethered construct exerted its effect via opening of the endogenous IP_3Rs, we performed experiments on DT40 cells in which all three forms of the IP_3R had been eliminated by homologous recombination (25). As shown in Fig. 4*A*, wild-type cells showed a cytoplasmic Ca^{2+} response to B cell receptor stimulation that acts via phospholipase C γ (PLCγ) and IP_3, whereas the TKO cells failed to respond to the same stimulation with a Ca^{2+} increase. Both wild-type and TKO cells showed a large Ca^{2+} increase to Tg but only a very small increase after the addition of caffeine (5–10 mM), the latter response being somewhat bigger in TKO cells (Fig. 4*A*). The Ca^{2+} response of transfected cells was studied in individual cells. Transfection of wild-type DT40 cells with the IP_3R LBD-ER construct has proven to be extremely toxic, with most cells undergoing apoptosis and only a very small fraction of

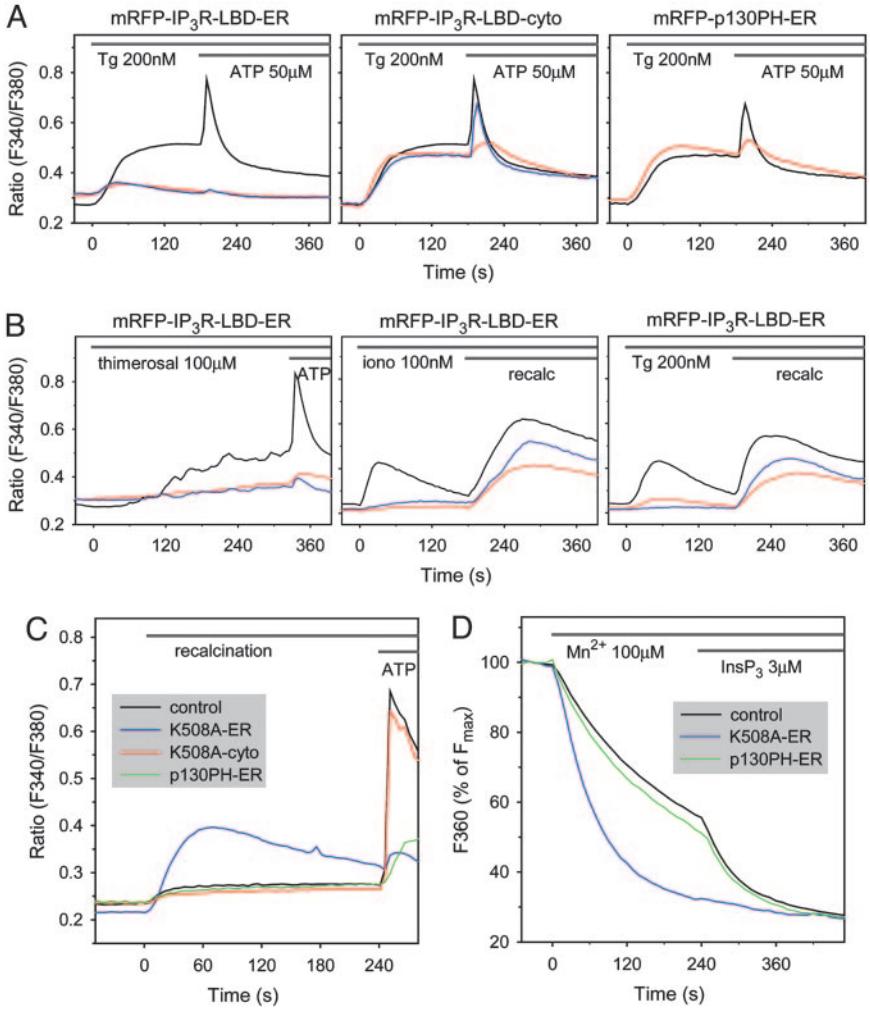

Fig. 3. Effect of ER-tethered IP_3 binding domains on the Ca^{2+} content of the intracellular Ca^{2+} pools. (*A*) Fura-2-loaded COS-7 cells transfected with the cytosolic (-cyto) or ER-tethered (-ER) forms of the indicated IP_3 binding domains (red) or their IP_3 binding deficient mutant forms (blue) were stimulated with 200 nM Tg and subsequently with 50 μM ATP. The average Ca^{2+} responses of cells expressing these constructs compared with those of untransfected cells (black) in the same fields are shown. (*Left*) Note that only the ER-tethered IP_3R LBD ER affects the amount of Ca^{2+} released by Tg and that IP_3 binding is not required for this effect. (*B*) Effects of expression of the ER-tethered IP_3R LBD on the response of cells to the IP_3-sensitizing agent, thimerosal (*Left*), or to a small concentration (100 nM) of ionomycin (*Center*) or Tg (*Right*) in the absence of external Ca^{2+}. The lack of response in cells expressing wild-type or mutant IP_3R LBD ER indicates that the Ca^{2+} pools are empty. Readdition of Ca^{2+} induces a large cytoplasmic [Ca^{2+}] increase reflecting the activation of the capacitative Ca^{2+} entry pathways. (*C*) Cells expressing the indicated constructs were incubated in Ca^{2+}-free medium (no added Ca^{2+} with 100 μM EGTA) for 8 min before readdition of 2.2 mM Ca^{2+} to the medium. The Ca^{2+} response of cells expressing the ER-targeted IP_3R LBD (K508A) (blue) was greatly increased, but cells expressing the cytosolic form of the IP_3R LBD (K508A) (red) or the ER-targeted p130PH (green) did not show increased Ca^{2+} entry. (*D*) Addition of Mn^{2+} to permeabilized cells quenched organelle-associated Fura-2 fluorescence at a significantly higher rate in cells expressing the ER-targeted IP_3R LBD than in control cells or in cells expressing the p130PH-ER construct. The former cells, unlike the latter, showed no further increase in response to IP_3, indicating the open state of the IP_3Rs.

transfected cells showing sufficient Fura-2 loading.[§] As observed in COS-7 cells, the Tg-induced Ca^{2+}-response was greatly impaired in these transfected cells (Fig. 4*B Left*). In contrast, many more of the TKO cells showed reasonable expression of the same construct, and the Tg-induced Ca^{2+} release in the transfected cells did not differ from that of their nontransfected counterparts (Fig. 4*B Right*). These data indicated that the IP_3R LBD-ER construct exerted its effect in the presence of endogenous IP_3Rs.

The All-Helical Fragment of the IP_3R LBD Is Sufficient to Open the IP_3R Channels. The recent solving of the crystal structure of the type I IP_3R LBD has revealed that it consists of an N-terminal β-domain forming a β-trefoil fold, hinged to an all-helical C-terminal domain containing three armadillo-repeat-like structures (26) (Fig. 5*A*). To determine whether these subdomains could still exert an effect, they were expressed separately and targeted to the outer surface of the ER. As shown in Fig. 5*B*, the ER-targeted N-terminal fragment containing only the β-sheets (224–423) had no effect on the Tg or ATP responses, whereas the effect of the C-terminal all-helical domain (427–605) was indistinguishable from that of the full-length LBD. Neither of these fragments had any effect when expressed in the cytosol, consistent with their inability to bind IP_3 (data not shown). Next, the IP_3R LBD was extended to include the N-terminal inhibitory sequences [IP_3R (1–605)]. The IP_3 binding affinity of this protein was significantly decreased (Fig. 5*C*), as noted by earlier reports (27). To determine the ability of this extended construct to impair agonist-induced Ca^{2+} signaling, its K508A mutant form

[§]Our explanation for the toxicity of the IP_3R LBD-ER construct in the wild-type cells is that its Ca^{2+}-releasing ability in the wild-type cells initiates an apoptotic program, whereas this effect is not manifested in the TKO cells because of the lack of IP_3Rs. However, the validity of this assumption was not pursued further in the present work.

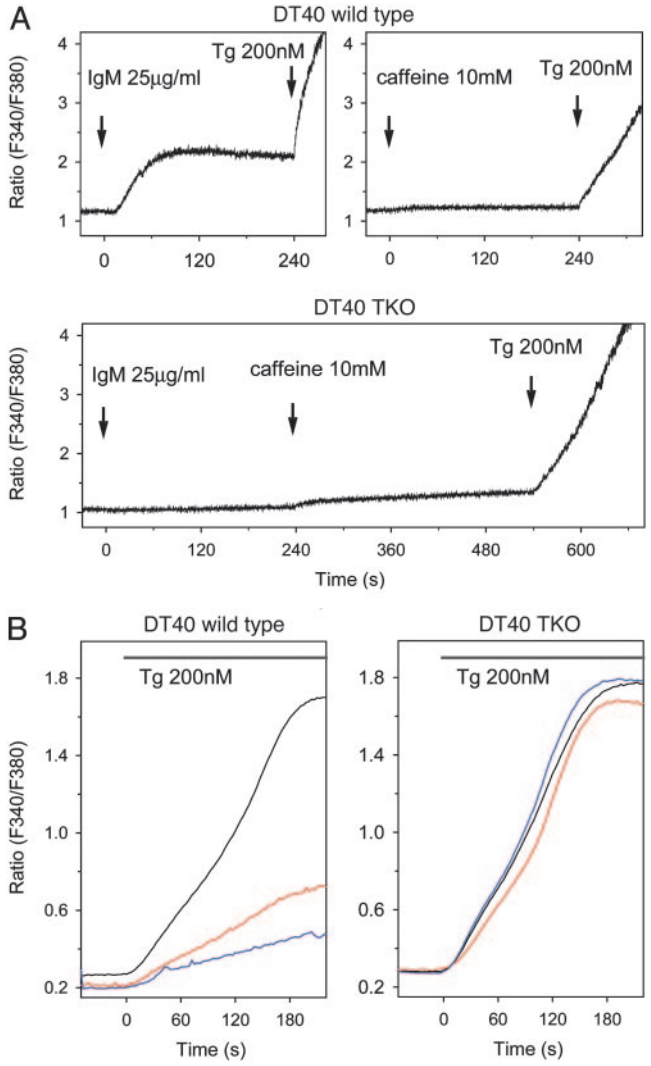

Fig. 4. Effect of ER-tethered IP_3 binding domains on the Ca^{2+} content of the intracellular Ca^{2+} pools in DT40 cells. Cytoplasmic Ca^{2+} responses of wild-type and TKO DT40 cells (lacking all three IP_3R isoforms) were studied in suspension (*A*) or as individual cells attached to glass coverslips (*B*). (*A*) Wild-type, but not TKO, cells showed a $[Ca^{2+}]$ increase in response to B cell receptor stimulation (IgM), and both cells showed a large $[Ca^{2+}]$ response to Tg, but only a very moderate $[Ca^{2+}]$ rise after caffeine (10 mM) treatment. The scale was chosen to accommodate the small caffeine responses, and, therefore, the Tg responses that reached a plateau at around a ratio of 6.5 in the cell suspension have been truncated. Wild-type and TKO DT40 cells were transfected with the wild-type (red) or mutant (blue) form of the IP_3R LBD ER by electroporation, and the individual cytoplasmic Ca^{2+} responses of transfected or untransfected (black) cells were measured after Tg treatment. (*B Right*) Note the lack of effect of the constructs in the TKO cells.

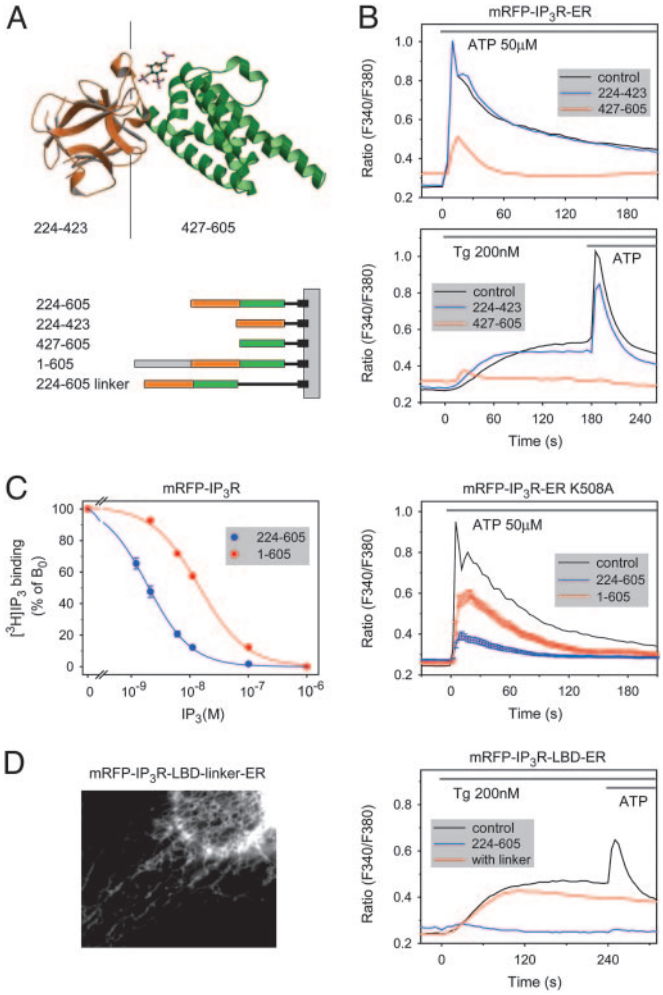

Fig. 5. The all-helical domain, but not the β-domain, of the IP_3R LBD is sufficient to empty the intracellular Ca^{2+} stores when tethered close to the surface of the ER. (*A*) The structure of the IP_3R LBD showing the β-domain (brown) and the all-helical armadillo-repeat-like domain (green) and schematic representation of the constructs used in these experiments. (*B*) Averaged Ca^{2+} responses of cells expressing the ER-tethered forms of the two isolated domains separately. Note the inhibitory effect of the all-helical domain, but not the β-domain, on Ca^{2+} release by ATP (*Upper*) or Tg (*Lower*). Also, the lack of delay in the peak $[Ca^{2+}]$ responses to ATP was consistent with the lack of IP_3 binding of the separated domains. (*C*) Effects of N-terminal extension of the IP_3R LBD (1–605) on the $[^3H]IP_3$ binding affinity of the recombinant proteins (*Left*), and effects of the expression of the K508A mutant of the N-terminally extended construct on the cytoplasmic $[Ca^{2+}]$ responses of COS-7 cells stimulated with ATP (*Right*). For comparison, the effects of the two constructs on the Ca^{2+} responses (±SEM) were calculated from cells that fell in the same range of expression (between 2,000 and 8,000 fluorescence arbitrary units) with an average of 4,222 ($n = 116$) and 4,516 ($n = 80$) for the 224–605 and 1–605 constructs, respectively. Note that the N-terminally extended LBD ER exerted a significantly smaller effect. (*D*) Extension of the distance of the IP_3R LBD from the ER surface by a rigid helical linker 9x(EAAAR) rendered the domain inactive in depleting the Ca^{2+} pools despite its ER localization (*Left*) and retained ability to interfere with the ATP-induced Ca^{2+} signal through IP_3 binding.

was used to prevent its IP_3-induced conformational change. As show in Fig. 5*C*, the potency of this N-terminally extended construct to empty the intracellular stores was significantly smaller than that of the shorter original construct when expressed at a similar level. Next we examined whether increasing the distance between the ER surface and the IP_3R LBD would affect the ability of the domain to exert its effect on the Ca^{2+} pools. As shown in Fig. 5*D*, including a rigid helical linker with nine turns almost completely abolished the Ca^{2+}-releasing effect of the construct despite its prominent ER localization, suggesting that the domain has to be within 50–60 Å (and probably even closer) to the ER surface to be active.

Together, these experiments demonstrated the ability of the all-helical region of the IP_3R LBD to increase the activity of the IP_3Rs when brought into its proximity by tethering to the surface of the ER. Without this tethering, even at the highest level of expression, no such effect could be observed, and even increasing its distance from the ER surface rendered the domain inactive. This effect did not require IP_3 binding and was greatly reduced by the

CELL BIOLOGY

addition of the N-terminal 1–223 sequence to the LBD. The small N-terminal fragment (1–223) has been shown to inhibit IP_3 binding (27), probably because of an interaction with the LBD and stabilization of its unliganded conformation. Our data also show that in this latter conformation the LBD is less capable of inducing release of Ca^{2+} from the ER. Together with reports demonstrating the proximity and physical interaction of the LBD with the IP_3R channel domain (15), the present observations may have implications for the possible gating mechanism of the IP_3R by its LBD (28). The truncated receptor containing only the transmembrane segments, i.e., the channel domain, was reported to be constitutively active, and deletion studies led to the conclusion that the channel is kept closed by the regulatory region that lies between the channel and the LBD (14). Current views suggest that IP_3 binding initiates a conformational change within the LBD that relieves the inhibitory effect of a yet unidentified segment of the regulatory region on the C-terminal tail of the protein that is considered to be the "gatekeeper" of the channel domain (28, 29). Our data suggest that unmasking of the all-helical segment of the LBD by IP_3 (probably with the concerted action of Ca^{2+}) could be part of the activation process.

We cannot rule out the possibility that expression of the LBD exerts its effect without direct interaction with the IP_3R itself, through interference with other proteins that regulate the endogenous IP_3Rs. Binding of most of the known IP_3R interacting partners have been localized to regions other than the LBD, but two proteins have been shown to interact with the LBD. One of them, IRBIT (IP_3R binding protein released by IP_3), binds to the LBD, but its binding is abolished by the K508A mutation (30). In our experiments, the K508A mutant was as potent as the wild-type in emptying the Ca^{2+} stores, making it unlikely that IRBIT sequestration would be responsible for the observed effects. The other protein(s) [calcium binding protein (CaBP)/caldendrin] belong to the family of small Ca^{2+}-binding proteins and have been shown to confer Ca^{2+} regulation to the receptor even without increases in IP_3 (31). Because these CaBPs are small soluble proteins, their binding to the expressed LBD would be expected to be similar whether the LBD is expressed in the cytosol or targeted to various distances from the ER surface. The strong steric requirements for the effect of LBD on channel opening makes it quite unlikely that the current observations would be the consequence of CaBP sequestration from the endogenous IP_3Rs and points to an interaction that needs to be very close to the surface of the ER, such as the channel domain itself.

The minimally active domain identified in the present study is the all-helical part of the LBD, which largely overlaps with the sequence identified in the Conserved Domain Architecture Retrieval Tool (CDART) database (www.ncbi.nlm.nih.gov/Structure/lexington/lexington.cgi) as the RIH domain (pfam01365) (RyR and IP_3R homology). Interestingly, two such domains are present in each subunit of the IP_3Rs and the RyRs, but only the IP_3Rs contain a suitable trefoil domain adjacent to their first RIH domain that supports IP_3 binding. The presence of two RIH domains in both the RyRs and IP_3Rs suggests that the observations presented in this study might be relevant to both of these closely related channel families, and our preliminary studies indicate that the RyR1 receptor RIH domain is also capable of emptying the Ca^{2+} stores when targeted to the ER. Although TKO DT40 cells have been reported to possess RyRs (32), their small caffeine response in this study indicates that they are not abundant in these cells. Therefore, the present studies could not conclusively answer the question of whether the IP_3R LBD could interact with RyRs. More studies will be needed to clarify these questions and to identify the exact mechanism by which the LBD may regulate the IP_3R channel domain. Nevertheless, the current experiments provide an experimental approach for further studies to better understand the gating mechanisms of this important Ca^{2+} channel family.

We thank Dr. Tomohiro Kurosaki (Department of Molecular Genetics, Institute for Liver Research, Kansai Medical University, Moriguchi, Japan) for the DT40 cells, Dr. Roger Y. Tsien (Department of Pharmacology and Department of Chemistry and Biochemistry, University of California at San Diego, La Jolla) for the mRFP, Dr. Suresh Joseph (Department of Pathology, Thomas Jefferson University, Philadelphia) for the anti-IP_3R antibody and the myc-tagged IP_3R construct, Dr. Gyorgy Hajnoczky for advice concerning the Mn^{2+}-quench experiments, and Judit Bakacsiné-Rácz for invaluable technical assistance. Part of the microscopy imaging (Zeiss 510) was performed at the Microscopy and Imaging Core (National Institute of Child Health and Human Development, National Institutes of Health) with the kind assistance of Drs. Vincent Schram and James T. Russell. P.V. and L.H. were supported by Hungarian Scientific Research Fund Grants OTKA T-034606 and OTKA T-046445, Medical Research Council Grant ETT 528/2003, and Hungarian National Committee for Technological Development Grants 02489/2000 and OTKA M036995.

1. Berridge, M. J. & Irvine, R. F. (1984) *Nature* **312,** 315–321.
2. Berridge, M. J., Lipp, P. & Bootman, M. D. (2002) *Nat. Rev. Mol. Cell Biol.* **1,** 11–21.
3. Mikoshiba, K. (1993) *Trends Pharmacol. Sci.* **14,** 86–89.
4. Galvan, D. L., Borrego-Diaz, E., Perez, P. J. & Mignery, G. A. (1999) *J. Biol. Chem.* **274,** 29483–29492.
5. Maeda, N., Kawasaki, T., Nakade, S., Yokota, N., Taguchi, T., Kasai, M. & Mikoshiba, K. (1991) *J. Biol. Chem.* **266,** 1109–1116.
6. Patel, S., Joseph, S. K. & Thomas, A. P. (1999) *Cell Calcium* **25,** 247–264.
7. Mignery, G. A. & Sudhof, T. C. (1990) *EMBO J.* **9,** 3893–3898.
8. Taylor, C. W. & Laude, A. J. (2002) *Cell Calcium* **32,** 321–334.
9. Hajnoczky, G., Robb-Gaspers, L. D., Seitz, M. B. & Thomas, A. P. (1995) *Cell* **82,** 415–424.
10. Li, W., Llopis, J., Whitney, M., Zlokarnik, G. & Tsien, R. Y. (1998) *Nature* **392,** 936–941.
11. Lewis, R. S. (2003) *Biochem. Soc. Trans.* **31,** Pt. 5, 925–929.
12. Tanimura, A., Nezu, A., Morita, T., Turner, R. J. & Tojyo, Y. (2004) *J. Biol. Chem.* **279,** 38095–38098.
13. Ramos-Franco, J., Galvan, D., Mignery, G. A. & Fill, M. (1999) *J. Gen. Physiol.* **114,** 243–250.
14. Nakayama, T., Hattori, M., Uchida, K., Nakamura, T., Tateishi, Y., Bannai, H., Iwai, M., Michikawa, T., Inoue, T. & Mikoshiba, K. (2004) *Biochem. J.* **377,** 299–307.
15. Boehning, D. & Joseph, S. K. (2000) *EMBO J.* **19,** 5450–5459.
16. Varnai, P., Lin, X., Lee, S. B., Tuymetova, G., Bondeva, T., Spat, A., Rhee, S. G., Hajnoczky, G. & Balla, T. (2002) *J. Biol. Chem.* **277,** 27412–27422.
17. Campbell, R. E., Tour, O., Palmer, A. E., Steinbach, P. A., Baird, G. S., Zacharias, D. A. & Tsien, R. Y. (2002) *Proc. Natl. Acad. Sci. USA* **99,** 7877–7882.
18. Takeuchi, H., Oike, M., Paterson, H. F., Allen, V. V., Kanematsu, T., Ito, Y., Erneux, C., Katan, M. & Hirata, M. (2000) *Biochem. J.* **349,** 357–368.
19. Uchiyama, T., Yoshikawa, F., Hishida, A., Furuichi, T. & Mikoshiba, K. (2001) *J. Biol. Chem.* **277,** 8106–8113.
20. Yang, M., Ellenberg, J., Bonifacino, J. S. & Weissman, A. M. (1997) *J. Biol. Chem.* **272,** 1970–1975.
21. Thastrup, O., Cullen, P. J., Drobak, B. K., Hanley, M. R. & Dawson, A. P. (1990) *Proc. Natl. Acad. Sci. USA* **87,** 2466–2470.
22. Putney, J. W., Jr. (1991) *Adv. Pharmacol.* **22,** 251–269.
23. Hajnoczky, G. & Thomas, A. P. (1994) *J. Biol. Chem.* **269,** 10280–10287.
24. Hajnoczky, G. & Thomas, A. P. (1994) *Nature* **370,** 474–477.
25. Sugawara, H., Kurosaki, M., Takata, M. & Kurosaki, T. (1997) *EMBO J.* **16,** 3078–3088.
26. Bosanac, I., Alattia, J. R., Mal, T. K., Chan, J., Talarico, S., Tong, F. K., Tong, K. I., Yoshikawa, F., Furiuchi, T., Iwai, M., *et al.* (2002) *Nature* **420,** 696–700.
27. Yoshikawa, F., Iwasaki, H., Michikawa, T., Furiuchi, T. & Mikoshiba, K. (1999) *J. Biol. Chem.* **274,** 328–334.
28. Taylor, C. W., daFonseca, P. C. & Morris, E. P. (2004) *Trends Biochem. Sci.* **29,** 210–219.
29. Uchida, K., Miyauchi, H., Furiuchi, T., Michikawa, T. & Mikoshiba, K. (2003) *J. Biol. Chem.* **278,** 16551–16560.
30. Ando, H., Mizutani, A., Matsu-ura, T. & Mikoshiba, K. (2003) *J. Biol. Chem.* **278,** 10602–10612.
31. Yang, J., McBride, S., Mak, D. O., Vardi, N., Palczewski, K., Haeseleer, F. & Foskett, J. K. (2002) *Proc. Natl. Acad. Sci. USA* **99,** 7711–7716.
32. Kiselyov, K., Shin, D. M., Shcheynikov, N., Kurosaki, T. & Muallem, S. (2001) *Biochem. J.* **360,** 17–22.